

THE PENNSYLVANIA STATE UNIVERSITY  
SCHREYER HONORS COLLEGE

DEPARTMENT OF ANIMAL SCIENCE

ROLE OF THE ARYL HYDROCARBON RECEPTOR IN ENDOMETRIUM OF DAIRY  
HEIFERS DURING THE ESTROUS CYCLE AND EARLY PREGNANCY

MICHELLE CHRISTINA HARTZELL  
SPRING 2016

A thesis  
submitted in partial fulfillment  
of the requirements  
for a baccalaureate degree  
in Animal Science  
with honors in Animal Science

Reviewed and approved\* by the following:

Troy L. Ott  
Professor of Reproductive Physiology  
Thesis Supervisor and Honors Adviser

Joy L. Pate  
Professor of Reproductive Physiology  
Faculty Reader

\* Signatures are on file in the Schreyer Honors College.

## ABSTRACT

Early embryonic loss in dairy cattle is a major economic cost to dairy producers. Our overall hypothesis is that a portion of these losses is mediated by aberrant response of the uterine immune system to the embryo. This research seeks to improve our understanding of a cellular mechanism that supports establishment of pregnancy. The aryl hydrocarbon receptor (AHR) is a ligand-activated transcription factor that reduces T cell proliferation and is involved in differentiation of T regulatory cells (Treg). We hypothesize that AHR-dependent Treg generation and inhibition of immune cell proliferation confers maternal immunosuppression toward the allogeneic embryo.

Holstein dairy heifers (n=22) were estrous synchronized and bred by artificial insemination (Day=0) or remained cyclic. Uterine endometrium was collected on day 17 of the estrous cycle (n=9), and days 17 (n=9) and 20 (n=4) of pregnancy. Total cellular RNA was isolated, converted to cDNA, and amplified by PCR using bovine AHR primers. A cDNA amplicon was visualized by gel electrophoresis, excised, and sequenced to determine its identity. Purified cDNA was used to generate a standard curve with a slope of -3.36, efficiency of 98.44%, and  $R^2$  of 0.997. Analysis of mRNA abundance for AHR was conducted using *RPL19* as the reference gene. Critical threshold data were adjusted for *RPL19* and  $2^{-\Delta Ct}$  values were analyzed using PROC Mixed and orthogonal contrasts. Although *AHR* was abundantly expressed in the endometrium, there was no difference in mRNA between pregnant and cyclic heifers nor between day 17 and day 20 pregnant heifers ( $P > 0.10$ ).

The presence of AHR protein in the endometrium was detected in all three groups studied by Western blot although the identity of all bands was not confirmed. Immunofluorescence analysis of uterine sections labelled with AHR antibody indicated AHR protein concentration

was greater in the shallow stroma ( $P = 0.05$ ) and tended to be greater in the myometrium ( $P = 0.06$ ) in day 17 and 20 pregnant heifers compared to day 17 cyclic heifers.

A dose response experiment of peripheral blood mononuclear cells (PBMC) cultured with kynurenine for 72 hours produced no measurable effect on total immune cell proliferation. However, individual immune cell types were not examined. This study confirms the presence of AHR mRNA and protein in the bovine endometrium during the estrous cycle and early pregnancy. Activation of this cellular receptor may initiate tolerogenic mechanisms that support early embryonic growth and development.

## TABLE OF CONTENTS

LIST OF FIGURES .....	iii
LIST OF TABLES .....	iv
ACKNOWLEDGEMENTS .....	v
LITERATURE REVIEW .....	1
Dairy Cattle Fertility .....	1
Endometrial-Conceptus Interaction.....	3
AHR-IDO Pathway .....	6
AHR in Reproductive Physiology.....	10
Focus of Present Thesis.....	11
MATERIALS AND METHODS.....	13
Sample Collection .....	13
RNA Extraction and cDNA Synthesis .....	13
Polymerase Chain Reaction and Gel Electrophoresis .....	14
Quantitative Polymerase Chain Reaction (qPCR) .....	15
Immunohistochemistry.....	16
Western Blot .....	17
Cell Culture and Flow Cytometry .....	18
RESULTS .....	21
Gel Electrophoresis and Sequencing.....	21
Quantitative Polymerase Chain Reaction (qPCR) .....	22
Western Blot .....	25
Immunohistochemistry.....	27
Flow Cytometry .....	29
DISCUSSION.....	31
CONCLUSIONS AND SIGNIFICANCE .....	35
APPENDIX.....	37
REFERENCES .....	38

**LIST OF FIGURES**

Figure 1: Milk Production and DPR (DCRC, 2009).....	2
Figure 2: Mechanism of ligand-activated AHR-dependent gene transcription.....	7
Figure 3: AHR ligand-dependent T cell differentiation.....	9
Figure 4: Products of PCR amplification reaction with AHR primers. ....	21
Figure 5: <i>AHR</i> Standard Curve with cDNA Standards and Unknowns (n=7) .....	22
Figure 6: <i>RPL19</i> Standard Curve .....	23
Figure 7: <i>AHR</i> Standard Curve with unknowns (n=22).....	24
Figure 8: Relative <i>AHR</i> expression in the endometrium of D17C, D17P, and D20P heifers. .	25
Figure 9: Image of polyacrylamide gradient gel electrophoresis with endometrial proteins...26	
Figure 10: Western blot of endometrial proteins incubated with anti-human AHR antibody. 27	
Figure 11: Representative uterine AHR immunofluorescent images.....	28
Figure 12: Percent area labeled for the AHR in uterine wall (UW), luminal epithelium (LE), shallow stroma (SS), shallow glands (SG), deep glands (DG) and myometrium (M). ....	29
Figure 13: Effects of kynurenine on PBMC proliferation with or without ConA. ....	30

**LIST OF TABLES**

Table 1: Critical threshold (Ct) values from <i>AHR</i> and <i>RPL19</i> qPCR .....	37
---	----

## ACKNOWLEDGEMENTS

I would like to acknowledge Dr. Troy Ott for everything he has done for me as a Schreyer Honors College scholar. I am grateful for the opportunity to become involved in undergraduate research and to complete my thesis in dairy cattle reproductive physiology. I also owe my gratitude to Sreelakshmi Vasudevan and Manasi M. Kamat for teaching me everything I have learned in the lab from fall 2014 through completion of my thesis. I could not have asked for better research mentors.

Thank you to the College of Agricultural Sciences Office of Undergraduate Education for allocating funding for my undergraduate research for the past three semesters. My appreciation also goes to Dr. Joy Pate and graduate students Lindy Steinberger, Camilla Hughes, and Molly Fetter for all of their assistance in completion of my project. I would also like to thank Dale Olver for all his support during my four years at Penn State. Lastly, I would like to acknowledge my parents, sister, and brother for inspiring me to follow in their footsteps to the College of Agricultural Sciences.

## LITERATURE REVIEW

### Dairy Cattle Fertility

Infertility is a significant source of economic loss for dairy producers and remains one of the primary reasons cows are culled from the herd (Bascom and Young, 1998). Manifestations of infertility in dairy cattle include lack of cyclicity, failure to conceive following breeding, early embryonic loss, and abortion. Infertility in a dairy herd depresses pregnancy rate, a key measure of reproductive performance of a dairy herd defined as the product of heat detection rate and conception rate. Conception rate indicates the frequency of conceptions among the total number of breedings performed. A dairy operation with a low conception rate uses a greater amount of resources including labor, feed, water, and veterinary services than a herd with a higher conception rate on average. For example, the number of replacement heifers needed to maintain herd size increases as fertility declines. Dairy cattle that fail to conceive after multiple breedings may be culled due to their low financial return relative to others in the milking herd. Farm profitability is therefore closely linked to reproductive performance, of which fertility is a primary determinant.

A large increase in average milk production per cow in the United States has occurred over the past 40 years, but this was accompanied by a substantial reduction in dairy cattle fertility (Gröhn and Rajala-Schultz, 2000). The decline in dairy cattle reproductive performance is evident by an increase in days open (DO), services per conception (SPC), and incidence of postpartum reproductive problems (Gröhn and Rajala-Schultz, 2000). To address declining fertility, a shift in genetic selection indexes has occurred in the last 15-20 years towards a stronger emphasis on reproductive traits, despite their low heritability (Hansen, 2007). In

artificial insemination (AI) proofs, the composite trait which most specifically reflects reproductive performance is daughter pregnancy rate (DPR). Daughter pregnancy rate is a function of days open (the time between parturition and conception) which is reported as pregnancy rate within a 21 day period (Weigel, 2006). The Dairy Cattle Reproduction Council indicates that breeding value for DPR has steadily increased since 2000 reflecting the current industry-wide emphasis on genetic selection for fertility (DCRC, 2009).

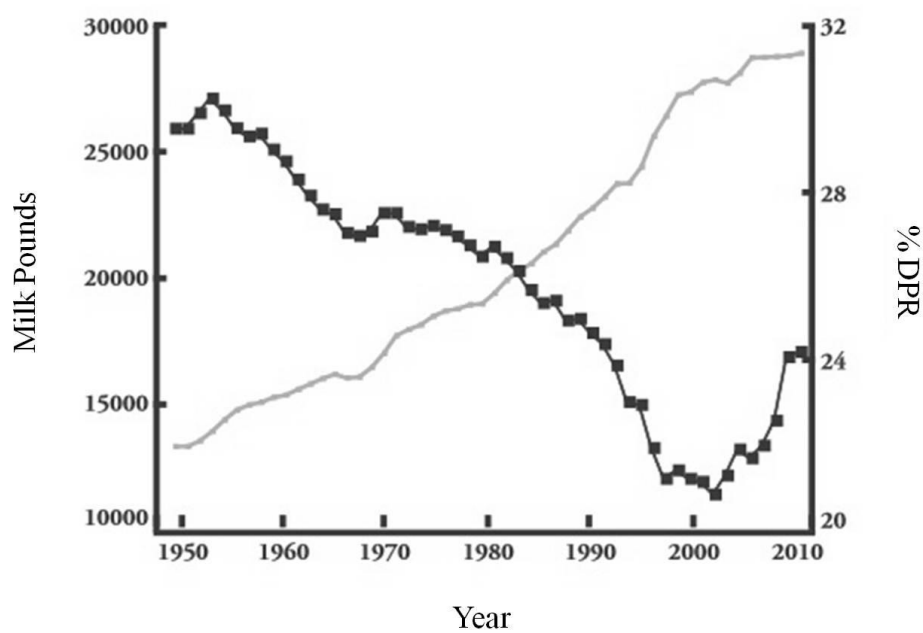


**Figure 1:** Milk Production and DPR (DCRC, 2009)

Despite the apparent negative association between milk production and fertility there is little evidence that high production *per se* is a significant cause of low fertility (Bello *et al.*, 2012). What high production does do is increase the demand for high quality animal management. Some of the highest milk production herds in the US also have high fertility. Therefore, efforts to improve fertility through genetics and reproductive management protocols of a dairy herd can be significantly influenced by on-farm management. Synchronization programs

and heat detection aids both represent modern technologies that facilitate early insemination of cows after the end of the voluntary waiting period. Precise breeding management is essential so farms have a steady supply of cows freshening and replacement calves. Furthermore, precise reproductive management is closely linked to production and helps maximize the proportion of the herd in peak lactation at any given time. Dairy cows peak in milk production 6-8 weeks following parturition before their production gradually declines throughout the remainder of their lactation. Peak milk is a strong predictor of 305 day milk production, and hence the average peak milk value for a dairy herd is another indicator of reproductive performance. As illustrated above, the effect of high fertility on dairy operations translates into greater milk revenue, net farm income, and an adequate supply of replacement heifers that represent the next generation of the milking herd. Thus, understanding the causes of infertility is important in the dairy industry to minimize financial losses from cows with poor reproductive performance.

### **Endometrial-Conceptus Interaction**

Early embryonic loss is a significant contributor to dairy cattle infertility. Embryonic mortality at any stage after conception results in financial loss from increased artificial insemination expenses in addition to costs related to maintenance of the nonpregnant cow. The later in gestation the embryonic loss occurs, the higher cost to the producer and increased likelihood that the cow will be culled from the herd. Embryonic mortality may occur at any point during gestation and is estimated to occur in 30% of all dairy cattle pregnancies (Vassilev *et al.*, 2005). When mortality occurs prior to day 24 of gestation, the event is characterized as early embryonic loss (Santos *et al.*, 2004). The period of early pregnancy is the most frequent

stage of embryonic mortality, with days 6 to 18 of gestation encompassing 65% of all estimated embryonic losses (Vassilev *et al.*, 2005).

The reasons for early embryonic mortality are not fully understood although genetic, nutritional, environmental, pathogenic, and cellular causes have been postulated. Genetic abnormalities that occur during embryogenesis, such as abnormal cell division, aneuploidy, polyploidy, or expression of lethal genes is responsible for a portion of embryonic losses (Geary, 2006). Heat stress is an environmental factor that contributes to embryonic loss in dairy cattle, defined as exposure to temperatures between 90-110°F and humidity greater than 40% (Geary, 2006). Somatic hyperthermia following breeding produces uterine ischemia and abnormal uterine prostaglandin  $F_{2\alpha}$  secretion, which may contribute to delayed embryonic development and subsequent mortality (Reynolds *et al.*, 1985; Putney *et al.*, 1989). During the transition period, cows enter a period of negative energy balance associated with a reduction in body condition. Loss of more than 1 point in body condition score (BCS) postpartum is associated with a depression in conception rate, increased calving interval, and increased risk of pregnancy loss (Walsh *et al.*, 2011). Furthermore, the bovine conceptus contains receptors for insulin-like growth factor-1 (IGF-1), whose physiological concentrations are influenced by energy balance and are in greater concentrations within the uterus of pregnant as opposed to cyclic dairy cattle (Kirby *et al.*, 1996).

Pathogens and disease status are additional factors that can cause early embryonic loss. Cows that develop clinical mastitis have higher services per conception and days open than healthy cows (Ahmadzadeh *et al.*, 2009). A reduction in immune function experienced by cows in negative energy balance during the transition period puts them at increased risk for metabolic and reproductive disorders, which subsequently affects reproductive performance. Postpartum

endometritis is associated with an increase in days open and a reduction in pregnancy rate (Fourichon *et al.*, 2000). Uterine infection, retained placenta, and dystocia during calving all increase the risk of a cow developing endometritis, hence reducing her fertility and putting her at risk for culling from the herd (LeBlanc, 2008). Several pathogenic diseases are also known to cause abortions in dairy cattle including Brucellosis, Leptospirosis, Bovine Viral Diarrhea, and Infectious Bovine Rhinotracheitis virus.

Additionally, early embryonic loss is attributed to abnormal or insufficient cellular communication between the conceptus and endometrium during embryogenesis and maternal recognition of pregnancy (MRP). Embryonic survival is highly dependent upon coordinated physiological interactions among the uterus, corpus luteum, and conceptus. Following fertilization, the morula stage of embryogenesis is initiated on day 4 of pregnancy, followed by migration of the embryo to the uterus and progression to the blastocyst stage. The embryo hatches from the zona pellucida on or before day 8 of gestation and elongates to take the form of a conceptus by day 14 (Santos and Ribeiro, 2014). Embryonic elongation and trophoblast cell proliferation is dependent upon histotrophe secretion by glands in the endometrial epithelium (Santos and Ribeiro, 2014). Prior to firm attachment of the conceptus to the endometrium starting on day 19 of gestation and subsequent placentation, a critical sequence of cellular and endocrine communication known as maternal recognition of pregnancy must occur. One of the best known MRP signals in ruminants is interferon tau (IFN- $\tau$ ). Interferon tau is secreted from the conceptus trophectoderm beginning on approximately day 15 of pregnancy (Brooks *et al.*, 2014). This results in rescue of the corpus luteum from destruction by uterine prostaglandin F<sub>2 $\alpha$</sub>  secretion and maintenance of progesterone production, which is essential for facilitating establishment and maintenance of pregnancy. During the periimplantation period, progesterone

secretion from the corpus luteum stimulates production of uterine histotrophe resulting in an increase in amino acids, glucose, cytokines, prostaglandins and other lipids and growth factors to support embryonic development (Brooks *et al.*, 2014). Interferon tau is also a key mediator of conceptus-endometrial interactions by stimulating gene expression in the endometrium and circulating immune cells (Ott and Gifford, 2010; Bazer *et al.*, 2012). Failure of the cellular and endocrine cross-talk during the blastocyst stage likely contributes to a substantial portion of the 33% of viable bovine embryos that fail to elongate and undergo placental attachment during early pregnancy (Santos and Ribeiro, 2014). The study of cellular communication during the early embryonic period may help reduce the observed rates of embryonic mortality observed in dairy cattle. Identification of the key proteins and regulatory molecules involved in facilitating embryonic growth and attachment to the endometrium is therefore an area of interest in reproductive physiology to understand why early embryonic loss occurs.

### **AHR-IDO Pathway**

The aryl hydrocarbon receptor (AHR) is a cytoplasmic protein found in complex with heat shock protein 90 (hsp90), cochaperone p23 (p23), and AHR-interacting protein (XAP2), which functions as a ligand-activated transcription factor (Baba *et al.*, 2005). The AHR gene is present in humans with its expression being highest in the placenta, lung, and liver (Jiang *et al.*, 2010). Toxicology studies elucidated AHR's role in physiological detoxification of xenobiotics. Aryl hydrocarbon receptor ligands including 2,3,7,8-tetrachlorodibenzo-p-dioxin (TCDD), 3-methylcholanthrene (3MC), and polychlorinated biphenyls (PCB) represent a potent class of carcinogenic aromatic compounds (Baba *et al.*, 2005). Upon binding by an environmental aryl

hydrocarbon, the AHR-ligand complex translocates to the nucleus, dimerizes with aryl hydrocarbon receptor nuclear translocator protein (ARNT), and associates with xenobiotic-responsive element (XRE) within the promoter of AHR target genes including *CYP1A*, *CYP1B1*, and *CYP1A2* (Hernandez-Ochoa *et al.*, 2008). These genes encode the oxidative detoxification enzymes cytochrome P450 1A1, 1B1, and 1A2 respectively (Nebert *et al.*, 2004). The aromatic structure of AHR ligands confers on them endocrine-disrupting capabilities that result in abnormal cell growth and altered homeostasis (Pocar *et al.*, 2005). Therefore, cytochrome P450-mediated detoxification prevents the abnormal physiological effects associated with exposure to aryl hydrocarbons.

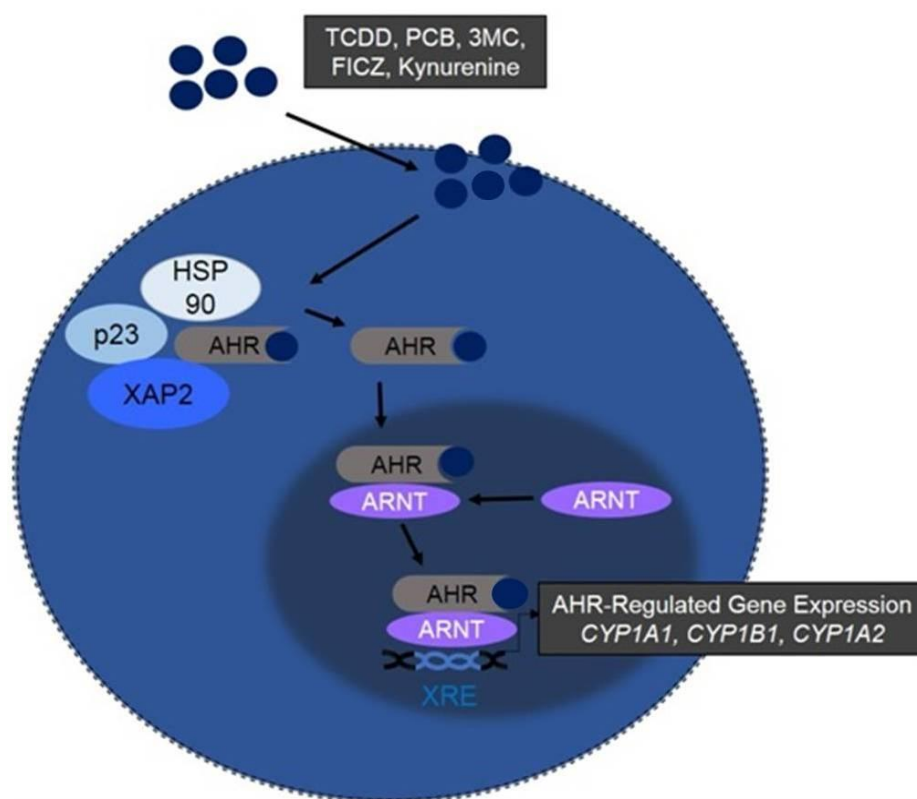


**Figure 2:** Mechanism of ligand-activated AHR-dependent gene transcription

The relatively recent advent of aryl hydrocarbon pollutants, byproducts from industrialization, suggests AHR has an endogenous physiological function in mammalian species. Furthermore, the protein is shown to be highly conserved across vertebrates and invertebrates alike (Baba *et al.*, 2005). Concurrent with this theory, endogenous ligands for AHR derived from nutrient metabolism have been identified. A tryptophan metabolite, kynurenine, and a cruciferous vegetable metabolite, 6-formylindolo[3,2-b]carbazole (FICZ), both serve as AHR ligands (Nebert *et al.*, 2004). Production of the kynurenine ligand is regulated by the activity of the indoleamine 2,3-dioxygenase (IDO) and tryptophan 2,3-dioxygenase (TDO) enzymes and the intracellular availability of tryptophan, an essential amino acid. With a variety of exogenous and endogenous ligands for AHR, the specific cellular effects produced by AHR activation are ligand-dependent.

In mouse models, activation of AHR by endogenous ligands has downstream effects on immune cell differentiation and proliferation into either proinflammatory or anti-inflammatory cell types. When AHR is activated by the kynurenine ligand, differentiation of naïve CD4<sup>+</sup> T cells into regulatory T cells (Treg) is induced, facilitated by transforming growth factor  $\beta$  (TGF- $\beta$ ) (Mezrich *et al.*, 2010; Shin *et al.*, 2013). Treg are negative regulators of the immune response and reduce the cytotoxic activity of T effector cells by suppressing proinflammatory cytokine secretion by T cells. Treg cells can be identified by the presence of forkhead box P3 (FOXP3<sup>+</sup>) transcription factor in the nucleus and the IL2 (CD25) surface receptor (Sakaguchi *et al.*, 2010). In murine cells, the presence of AHR in T cells is necessary for optimal FoxP3<sup>+</sup> expressing Treg generation *in vitro* (Mezrich *et al.*, 2010). In contrast to the anti-inflammatory pathway, FICZ binding to AHR induces proliferation of T helper 17 (T<sub>H</sub>17) cells (Mezrich *et al.*, 2010). The growth factors interleukin-6 (IL-6) and transforming growth factor  $\beta$  (TGF- $\beta$ ) are involved in

differentiation of  $T_H17$  cells, which secrete proinflammatory cytokines including interleukin-17 (IL-17) and interleukin-22 (IL-22) (Shin *et al.*, 2013; Stevens and Bradfield, 2008). Therefore, differentiation of naïve T cells into the proinflammatory  $T_H17$  or anti-inflammatory Treg phenotype is controlled by which growth factors and AHR ligands are present in the cellular microenvironment.

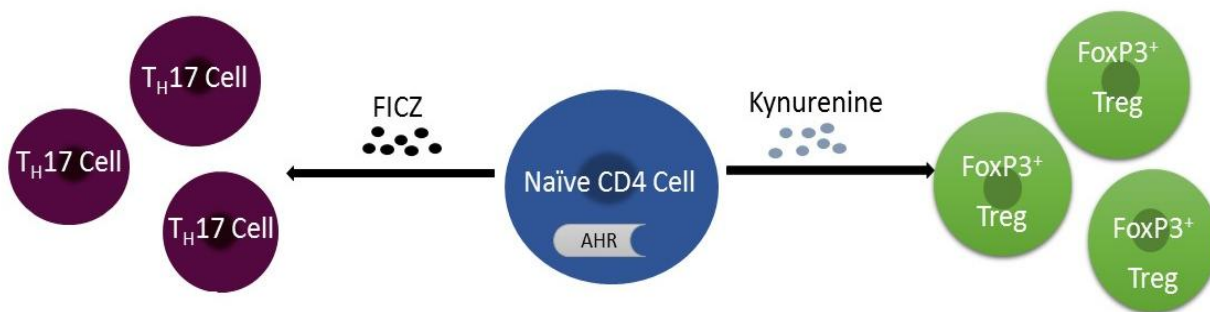


**Figure 3:** AHR ligand-dependent T cell differentiation

The effect of AHR activation on differentiation of leukocyte phenotypes with opposing immunological roles is highly dependent on the type of receptor ligand present. As a result of the effect of AHR activation to suppress effector T cells and generate Treg, this transcription factor is widely studied in cancer biology, transplant medicine, and autoimmune diseases. The AHR-IDO pathway suppresses cell-mediated anti-tumor responses by preventing the proliferation of effector T cells that target tumor cells in cell-mediated immunity. Pharmacological inhibition of IDO is of current interest in cancer immunotherapy to inhibit this immunosuppressive pathway in cancer patients as well as in immunocompromised graft-transplant patients (Munn *et al.*, 2007).

## **AHR in Reproductive Physiology**

The role of the immune system in modulating pregnancy is highly relevant to the issue of embryonic loss. By possessing one half paternal and one half maternal DNA, the semiallogeneic conceptus is recognized as immunologically dissimilar by the maternal immune system. Hence, innate immune reaction to the conceptus via proinflammatory leukocytes and cytokines could contribute to early embryonic losses in dairy cattle. The AHR-IDO pathway may be active in reproductive tissue to support an environment of immune tolerance. A review of AHR in reproductive physiology studies across several species supports a role for this transcription factor in preimplantation uterine physiology. Expression of aryl hydrocarbon receptor mRNA has not been characterized in bovine reproductive tissues other than in the oocyte and cumulus cells, where it was detected but not characterized (Pocar *et al.*, 2003). The AHR mRNA and protein were detected in human, mouse, and rat uteri (Hernandez-Ochoa *et al.*, 2008, Kluxen *et al.*, 2011). Concentration of AHR mRNA was higher in pregnant midgestational mice compared to nonpregnant mice, suggesting a physiological purpose for AHR during pregnancy (Hernandez-Ochoa *et al.*, 2008). In the human uterus, AHR mRNA is present in the cytoplasm of epithelial cells of endometrial glands and in both the cytoplasm and nucleus of stromal cells during the proliferative menstrual phase (Hernandez-Ochoa *et al.*, 2008). Similar findings in the endometrium of pregnant rabbits show AHR is present in the nucleus of glandular epithelial cells, but in nonpregnant rabbits was localized within the cytoplasm of these cells (Hernandez-Ochoa *et al.*, 2008). The presence of AHR protein in the nucleus during the preimplantation phase of embryonic development indicates the AHR-ligand complex is transcriptionally active, because the complex translocates to the nucleus when bound by one of its ligands.

Based on the role of AHR in generating Treg and suppressing effector T cell proliferation, activation of this receptor may support the establishment of an immunologically tolerogenic environment in the uterus that is conducive to early embryonic growth and development. Treg numbers increase in the uterus during early pregnancy in primates (Ruocco, *et al.*, 2014). FoxP3<sup>+</sup> transcription factor, a marker for Treg, is detected in human endometrial biopsies of healthy pregnant women and concentrations of the protein were reduced in women suffering from infertility (Ruocco *et al.*, 2014). Infertile women and women suffering from recurrent spontaneous abortions (RSA) have fewer Treg or a defective population of Treg in the uterus, suggesting a close link between these cells and successful establishment of pregnancy (Ruocco, *et al.*, 2014). In mouse studies, inhibition of IDO with 1-methyl-tryptophan resulted in high rates of fetal abortion (Cady *et al.*, 1991). This is consistent with a role for AHR in the generation of Treg in mice via IDO-dependent kynurenine production, indicating the IDO-AHR network may be active in the mammalian uterus (Mezrich *et al.*, 2010). Furthermore, AHR knockout mice exhibit compromised fertility and a higher rate of embryonic mortality (Abbott *et al.*, 1999). In summary, expression of the AHR in reproductive tissues and the association of infertility with Treg deficiency may indicate a critical role of the AHR-IDO pathway in mammals during pregnancy.

### **Focus of Present Thesis**

The focus of this research is to understand the role of AHR in the immunology of early pregnancy. By comparing AHR expression between pregnant and cyclic heifers, we can better understand if it contributes to development of an immunosuppressive environment in the

endometrium through the IDO-AHR pathway. The results from this project are relevant to identifying key cell types and molecules involved in establishing a tolerogenic environment for the embryo during early pregnancy. Studying AHR abundance and localization during the earliest stages of conceptus signaling should contribute to a more complete understanding of the role of the IDO enzyme. Previous work from our lab showed that IDO mRNA was expressed 15 fold higher in the endometrium of pregnant dairy heifers compared to cyclic heifers. Furthermore, IDO protein is present in higher concentrations in the endometrium of day 17 pregnant heifers compared to cyclic heifers on day 17 of the estrous cycle. Based on the role of IDO in AHR activation, we hypothesize that AHR mRNA will be expressed in the bovine endometrium with its expression higher in pregnant heifers than cyclic heifers or that pregnancy will result in changes in the distribution of AHR expression across the uterine wall or within cells. For example, activation of the AHR should result in translocation from the cytoplasm to the nucleus. Finally, based on the known effect of kynurenine on AHR-dependent effector cell proliferation, we hypothesize that bovine uterine peripheral blood mononuclear cells (PBMC) cultured with this metabolite will exhibit a reduction in proliferation relative to controls.

It will be determined if AHR is present in the endometrium and if differences in its expression exist between pregnant and cyclic dairy heifers. Furthermore, this project seeks to determine if kynurenine has an effect on immune cell proliferation.

## **MATERIALS AND METHODS**

### **Sample Collection**

All activities involving animals were approved by the Pennsylvania State University Institutional Animal Care and Use Committee guidelines outlined in protocol #44524. Commercial dairy heifers (250-450 kg) were randomly assigned to three groups according to pregnancy status; heifers at day 17 of the estrous cycle (D17C; n=9), day 17 of pregnancy (D17P; n=9), and day 20 of pregnancy (D20P; n=4). Heifers were estrous synchronized using two intramuscular prostaglandin F<sub>2α</sub> injections (2 cc, Lutalyse<sup>®</sup>, Zoetis, Kalamazoo, MI). Upon visual detection of estrus, heifers assigned to the day 17 and day 20 pregnancy groups were artificially inseminated 12 hours and 24 hours later (D=0). Heifers were euthanized according to group assignment on day 17 (D=17) or day 20 (D=20) by captive bolt at a USDA inspected abattoir and the uterus was immediately recovered. Blood samples were collected at slaughter and assayed for progesterone by enzyme linked immunosorbent assay (ELISA). The uterus was flushed with 40 mL ice cold phosphate buffered saline to confirm the presence of a conceptus. Endometrium (5 g) was dissected free from myometrium and snapfrozen in liquid nitrogen for later RNA isolation. Full thickness uterine biopsies were generated using an 8 mm cork borer and were preserved in Optimal Cutting Temperature matrix (OCT; Miles Laboratories, Inc., Elkhart, IN) in isopentane cooled over liquid nitrogen.

### **RNA Extraction and cDNA Synthesis**

A tissue homogenizer (Unidrive X1000 Homogenizer Drive, Paso Robles, CA) was treated with RNase AWAY (Molecular BioProducts, San Diego, CA) prior to RNA extraction.

Endometrial tissue (0.1g) was homogenized in 1 mL TRIzol (Invitrogen, Carlsbad, CA) for approximately 3-4 minutes (4000 RPM) and total cellular RNA extraction was performed according to manufacturer's instructions. Between tissues the blade was treated with RNase AWAY followed by three sequential washes in 80%, 90%, and 100% ethanol. Preliminary products of RNA extraction were evaluated for nucleic acid quality and quantity using an Experion Automated Electrophoresis System (Bio-Rad, Hercules, CA). All RNA samples were then treated with DNase (RQ1 RNase-free DNase kit; Promega, Madison, WI) according to the manufacturer's instructions. One microgram of RNA was converted to cDNA (Dynamo cDNA Synthesis Kit, Thermo Fisher Scientific, Carlsbad, CA) according to the manufacturer's protocol.

### **Polymerase Chain Reaction and Gel Electrophoresis**

Forward and reverse primers for the aryl hydrocarbon receptor were designed using NCBI primer basic local alignment search tool (BLAST). Complementary DNA was diluted 1:5 with nuclease-free water (Ambion, Carlsbad, CA) and 5  $\mu$ L was combined with 1  $\mu$ L dNTP mix (Promega, Madison, WI), 0.25  $\mu$ L GoTaq polymerase (Promega, Madison, WI), 10  $\mu$ L SYBR green (SensiMix SYBR No-ROX kit; Biorline, Taunton, MA), 3  $\mu$ L of forward and reverse AHR primers (15  $\mu$ M, Eurofins MWF Operon, Huntsville, AL) and 27.75  $\mu$ L nuclease free water. The amplification reaction was run using a PTC-200 DNA Engine Cycler (Bio-Rad, Hercules, CA) under the following conditions; a 95°C denaturation step for 5 minutes, 60°C annealing for 45 seconds, 72°C elongation for 1 minute, and a final 72°C elongation step for 5 minutes which repeated for 40 cycles. The products of PCR amplification were stored at -20°C for subsequent gel electrophoresis analysis. A mixture containing 1.25 g agarose (Invitrogen, Carsbad, CA), 17

mL 5X TAE (0.1M Tris base, 0.004M Na<sub>2</sub>EDTA<sub>2</sub>, 0.0634M acetic acid, 1L distilled water, pH 8.5) and 67 mL distilled water was heated to boiling then cooled at room temperature. During cooling, 8.24 μL ethidium bromide (Invitrogen, Carlsbad, CA) was added and the mixture was poured in a medium gel box once it reached approximately 50°C. A 20 μL sample of 1 Kb Plus DNA ladder (Invitrogen, Carlsbad, CA), was loaded in the first well. The products of the PCR reaction (n=11) and nuclease free water were loaded into the remaining wells. The electrophoresis was conducted for 1 hour at 90V. Amplicons were visualized using a ChemiDoc XRS system (Bio-Rad, Hercules, CA) under ultraviolet transillumination. The amplicon from heifer #702 (D20P) was excised from the gel and purified (QIAquick Gel Extraction Kit, Valencia, CA) according to the manufacturer's protocol. Sequence analysis of the amplicon was performed at the Penn State Nucleic Acid Core Facility (Huck Institutes of the Life Sciences, Pennsylvania State University, University Park, PA).

### **Quantitative Polymerase Chain Reaction (qPCR)**

Serial dilutions ( $10^{-1}$  to  $10^{-12}$ ) of cDNA samples were prepared in nuclease free water for development of a qPCR standard curve. Standards (2μL) were combined with 10 μL SYBR Green master mix, 0.33 μL AHR forward and reverse primers (15μM) and 7.34 μL nuclease free water. Samples of cDNA (5 μL) from heifers (n=7) were amplified using the same protocol with 3.34 μL nuclease free water to a total volume of 20 μL for all standards and samples. The qPCR plate was centrifuged at 1,800 rpm for 30 seconds. Real time polymerase chain reaction was performed on a 7500 Fast System Real Time PCR machine (Applied Biosystems, Foster City, CA) using the cycling conditions described above. Following validation of the assay by a

standard curve, the qPCR procedure was repeated with cDNA from the entire sample of heifers (n=22) in duplicates. An identical protocol was followed for the reference gene *ribosomal protein L19 (RPL19)* to generate reference Ct values for AHR qPCR statistical analysis.

### **Immunohistochemistry**

A microtome was used to generate tissue sections (5µm) from full thickness uterine wall biopsies preserved in OCT for heifers (n=5) in each experimental group (D17P, D17C, D20P). Two sections per animal were transferred to an adhesive microscope slide and frozen (-80°C). At the time of analysis, slides were incubated for 30 minutes at 37°C followed by an ice cold pure acetone wash for 10 minutes. Two subsequent washes in 1X PBS (0.137M NaCl, 2.7mM KCl, 4.3mM Na<sub>2</sub>HPO<sub>4</sub>, 1.47mM KH<sub>2</sub>PO<sub>4</sub>) were performed for 5 minutes followed by a 30 minute permeabilization in diluent (1X PBS, 0.1% BSA (EMD Millipore, San Diego, CA), 0.1% Triton X-100 (Sigma Aldrich, Saint Louis, MO). Slides were incubated overnight in a 4°C humidified chamber with a 1:200 dilution of AHR mouse anti-human monoclonal antibody (MA1-514, Thermo Fisher Scientific, Rockford, IL) or mouse IgG1 negative isotype antibody (MCA928, AbD Serotec, Raleigh, NC) in diluent and 20% goat serum (Sigma-Aldrich, St. Louis, MO). Following overnight incubation, slides were incubated for one hour in the dark with a 1:200 dilution of anti-IgG Alexa Fluor 555 secondary antibody (A-21422, Invitrogen, Carlsbad, CA) in diluent and 20% goat serum in a humidified chamber. Two final washes for 10 minutes each were performed in diluent followed by addition of 15 µL of 4',6-diamidino-2-phenylindole (DAPI; Invitrogen, Carlsbad, CA) per section. Sections were covered by a microscope slide and stored in the dark overnight for subsequent viewing under an Olympus BX-51 fluorescent

microscope (Olympus, Tokyo, Japan) equipped with an Olympus XX camera and DP71 image capture software. Images of Alexa Fluor 555 (AF555) secondary antibody and DAPI nuclei staining were captured at 40X magnification with exposure being kept constant for all images. Three images of secondary antibody and DAPI staining in the luminal epithelium (LE), shallow stroma (SS), shallow glands (SG), deep glands (DG), and myometrium (M) were captured and merged for each tissue region for each heifer. Average labeling intensity and percent area of each tissue section labeled was quantified using NIH ImageJ software.

### **Western Blot**

Protein was isolated from samples of uterine endometrium (n=6) and concentration was determined using a BCA Protein Assay Kit (Thermo Fisher Scientific, Rockford, IL). Murine in vitro translated AHR protein served as a positive control (Kindly provided by Dr. Perdew, Penn State University) and a murine tissue lysate with AHR protein extracted served as the negative control. Protein (50 $\mu$ g) samples were combined with 10 $\mu$ L sample buffer (7.5mL distilled water, 760mg Tris base, 2g sodium dodecyl sulfate (SDS), 10mL glycerol, 5mL 2-beta mercaptoethanol, 300 $\mu$ L bromphenol blue) and nuclease free water. Samples were incubated for 5 minutes at 95°C then cooled to room temperature for 1 minute. Wells in two Mini-PROTEAN TGX Precast Gels (Bio-Rad, Hercules, CA) containing 1X electrode buffer (30.3g Tris base, 144.2g glycine, 10g SDS, 900mL distilled water, pH 8.3) were loaded with 30 $\mu$ L of samples. Additional wells received 10  $\mu$ L Precision Plus Protein All Blue Standards (Bio Rad, Hercules, California). Sample proteins were separated on the gel for approximately 60 minutes at 70mA. Proteins on one gel were transferred using an iBlot Dry Blotting System (Invitrogen, Rockford,

IL) onto a nitrocellulose membrane and the remaining gel was incubated with 1.25 g coomassie brilliant blue R-250 dye (Thermo Fisher Scientific, Rockford, IL), 400 mL 95% ethanol, 70 mL glacial acetic acid, and 540 mL distilled water for one hour then washed in destain (400mL 95% EtOH, 70mL glacial acetic acid, 530mL distilled water) overnight. The nitrocellulose blotted membrane underwent a 2 hour incubation with 50 mL TBST (20mL 1M Tris, 137mL 1M NaCl, 500 $\mu$ L Tween 20, 843mL distilled water) and 2.5 g BSA followed by an overnight incubation at 4°C with a 1:500 dilution of primary mouse anti-human AHR antibody (concentration unknown, MA1-514, Thermo Fisher Scientific, Rockford, IL) in 5 mL TBST and 0.02% BSA. Four 5 minute washes with TBST were performed and the membrane was slow rocked for 1 hour with a 1:1000 dilution goat anti-mouse IgG horseradish peroxidase secondary antibody (0.8mg/mL, Thermo Fisher Scientific, Rockford, IL) prior to four 10 minute TBST washes. SuperSignal West Femto Maximum Sensitivity Substrate (Thermo Fisher Scientific, Rockford, IL) was applied to the membrane in the dark according to manufacturer's instructions. A ChemiDoc XRS system (Bio-Rad, Hercules, CA) was used to visualize the AHR bands and Quantity One 1-D Analysis Software was employed to capture images of the membrane.

### **Cell Culture and Flow Cytometry**

Approximately 150 mL of whole blood was obtained from the jugular vein of a day 11 (D11C) cyclic heifer, combined with 2 mL PBS-EDTA (0.1L 10X PBS, 4mL 2mM EDTA, 900mL distilled H<sub>2</sub>O), and stored on ice. Blood (12-13 mL) was aliquoted into borosilicate glass tubes, covered, and centrifuged at 1513 x g for 15 minutes at 4°C. Buffy coats were recovered and combined with ice cold PBS-EDTA to a total volume of 4 mL, which was layered on top of

3 mL Ficoll Paque PLUS (GE Healthcare, Piscataway, NJ) and centrifuged at 648 x g for 30 minutes at 25°C. The dense mononuclear band was collected and suspended in 8-10 mL PBS-EDTA and centrifuged at 640 x g for 10 minutes at 4°C. The pellet was set aside from the supernatant which was centrifuged at the same conditions to obtain an additional pellet. The two pellets were pooled, resuspended in 15 mL PBS-EDTA and centrifuged three times at 288 x g followed by 128 x g and 98 x g for 10 minutes each at 4°C. The resulting pellet of peripheral blood mononuclear cells (PBMC) was resuspended in 2 mL PBS-EDTA. A 3 µL sample of a 1:10 dilution of PBMC in PBS-EDTA was treated with 27 µL Trypan Blue Stain (Gibco, Life Technologies, Carlsbad, CA) and cell viability and number was determined using a hemocytometer. PBMC were set aside for unlabeled and CFSE controls. A fraction of PBMC isolated ( $14 \times 10^6$  cells) were combined with 1333 µL RPMI-1640 medium (Life Technologies, Grand Island, NY) containing 0.2% gentamicin (2 mg/mL; Gibco, Life Technologies, Carlsbad, CA), and 0.1% Insulin-Transferrin-Selenium (ITS; 100 mg/mL, Gibco, Carlsbad, CA). The 2 mL suspension was incubated with 7 µL of a 1:3 dilution of carboxyfluorescein succinimidyl ester (CFSE; Sigma Aldrich, Saint Louis, MO) in sterile PBS in the dark for 15 minutes at 37°C followed by 10 minutes at room temperature. Unincorporated CFSE was removed with three 10 minute 295 x g washes in 2 mL Ham F12 (Thermo Fisher Scientific, Carlsbad, CA) with 10% fetal bovine serum (FBS; Gibco, Carlsbad, CA) at 4°C. The final pellet was resuspended in 2 mL of RPMI-1640 containing 0.1% ITS, and 0.2% gentimicin. CFSE labeled cells (500,000 cells/well) were added to a 96 well plate (Corning Costar, Corning, NY) in duplicates along with duplicate CFSE control wells and unlabeled control wells. Dilutions of kynurenine (2.5mM, Sigma Aldrich, Saint Louis, MO) were added to CFSE-labeled cells to achieve concentrations of 0 µM, 25 µM, 50 µM, 100 µM, 200 µM, and 400 µM in duplicate wells. One set of wells

containing CFSE-labeled cells with kynurenine was cultured with 1  $\mu$ L Concanavalin A (Con A; 8 $\mu$ g/ $\mu$ L, Calbiochem, San Diego, CA) and served as a positive control for proliferation. Cells were cultured for 72 hours in an incubator at 37°C. A Guava EasyCyte Plus (EMD Millipore, Billerica, MA) flow cytometer was used to measure CFSE staining intensity as a measure of proliferation and staining was analyzed using FlowJo software.

## RESULTS

### Gel Electrophoresis and Sequencing

The fluorescent amplification products of the polymerase chain reaction for AHR were visualized at the expected 164 bases (Figure 4).

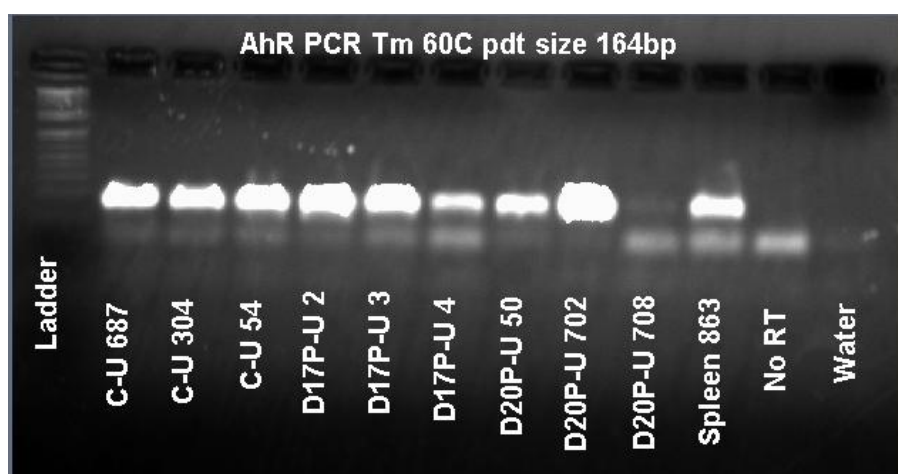


**Figure 4:** Products of PCR amplification reaction with AHR primers. The amplicon was evident at the expected 164 base pairs.

The amplification product from one sample (D20P-#702) was excised and sequenced to confirm the presence of AHR gene in the amplicon. Sequence analysis using National Center for Biotechnology Information (NCBI) Basic Local Alignment Search Tool (BLAST) revealed 97% sequence similarity of the forward and reverse cDNA sequence to *Bos taurus* aryl hydrocarbon receptor (AHR) gene (NCBI Gene #280714).

## Quantitative Polymerase Chain Reaction (qPCR)

The qPCR assay using AHR primers was validated using a 12 log dilution of AHR cDNA. The standard curve exhibited of slope of -3.36, 98.44% efficiency, and  $R^2$  of 0.997 (Figure 5). All unknown cDNA samples (n=7) amplified with AHR primers during development of the standard curve fell within the measurable range of the assay.

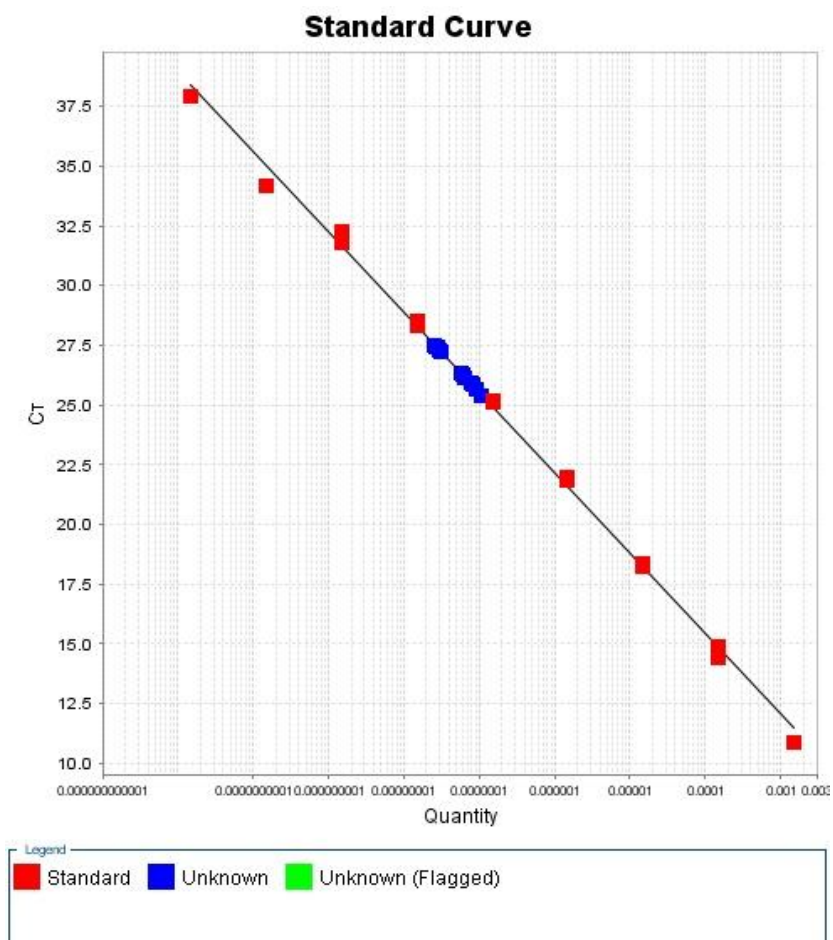


**Figure 5:** *AHR* Standard Curve with cDNA Standards and Unknowns (n=7)

A qPCR assay for the *RPL19* reference gene was also validated using a 12 log dilution curve of an RPL19 amplicon. The standard curve had a slope of -3.22, efficiency of 95.9% and an  $R^2$  of 0.998 (Figure 6).

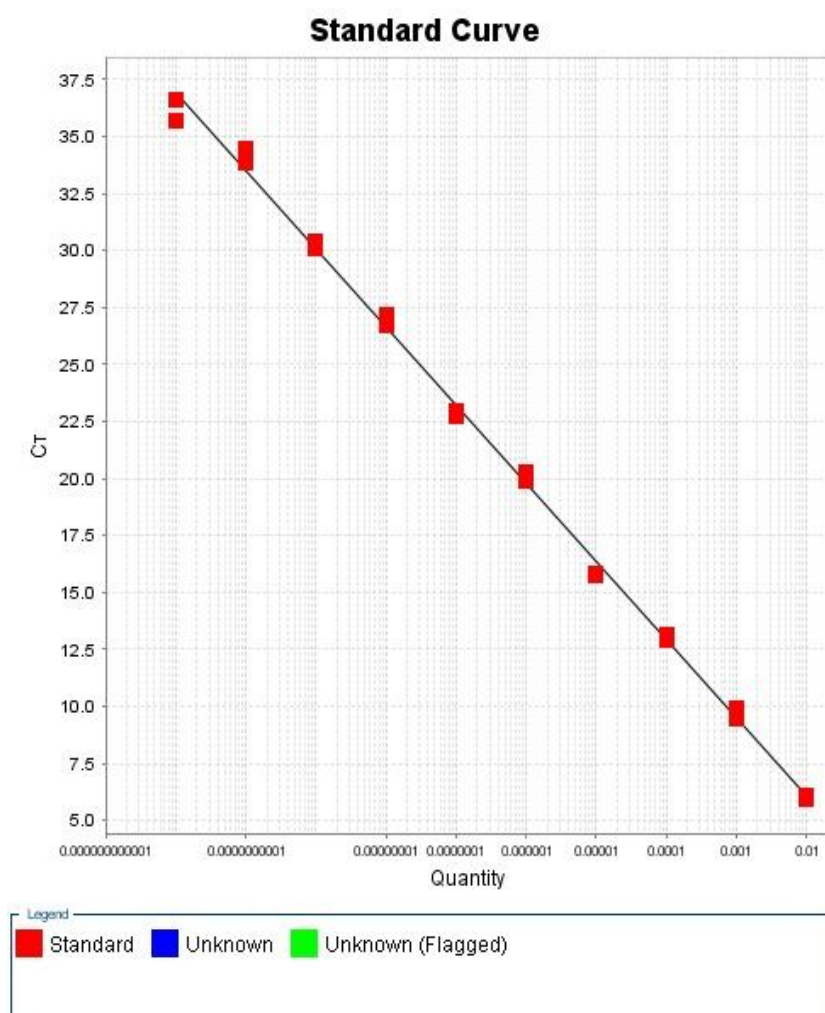


**Figure 6:** *RPL19* Standard Curve

Amplification of the entire sample size of unknowns (n=22) with *AHR* standard dilutions generated an amplification plot of slope -3.19, efficiency of 105.68% efficiency and  $R^2$  of 0.996 (Figure 7). A single melting curve was observed for all samples and standards.

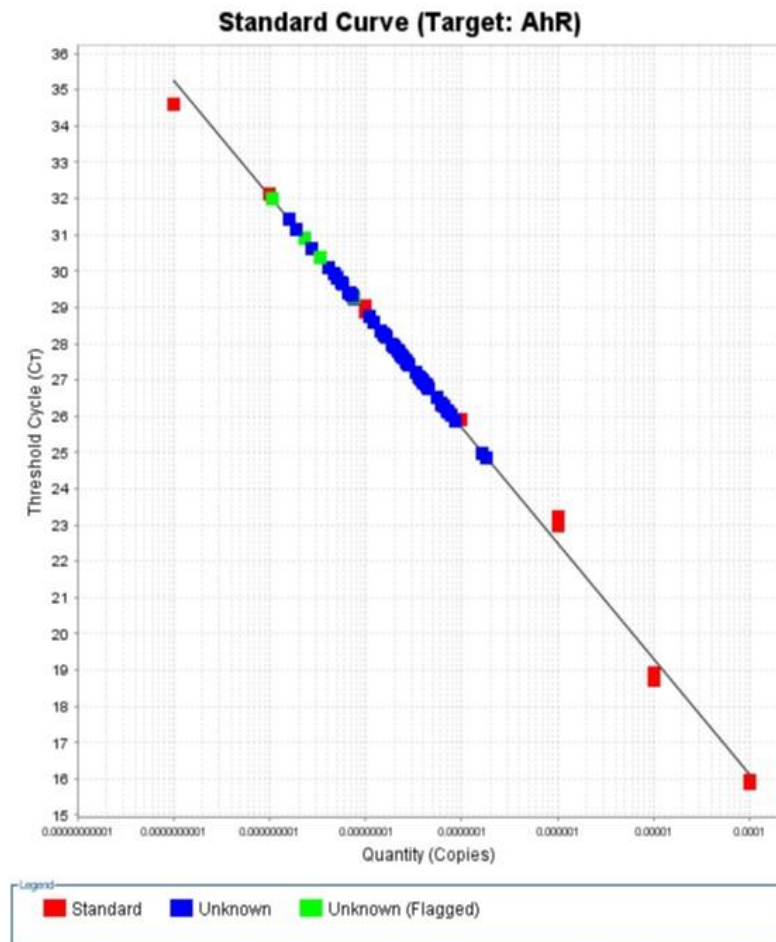


**Figure 7:** *AHR* Standard Curve with unknowns (n=22)

Steady-state mRNA abundance for *AHR* in the endometrium was determined by analyzing critical threshold (Ct) values determined by quantitative polymerase chain reaction. Statistical analysis of *AHR* expression was conducted using *RPL19* as the reference gene (Ct values in Appendix 1). Critical threshold data were adjusted for *RPL19* and  $2^{-\Delta Ct}$  values were

analyzed using PROC Mixed and status effects tested using orthogonal contrasts (cyclic v pregnant and day 17 pregnant v day 20 pregnant). There was no difference in *AHR* mRNA abundance between pregnant and nonpregnant heifers nor between day 17 and day 20 pregnant heifers ( $P > 0.10$ , Figure 8).

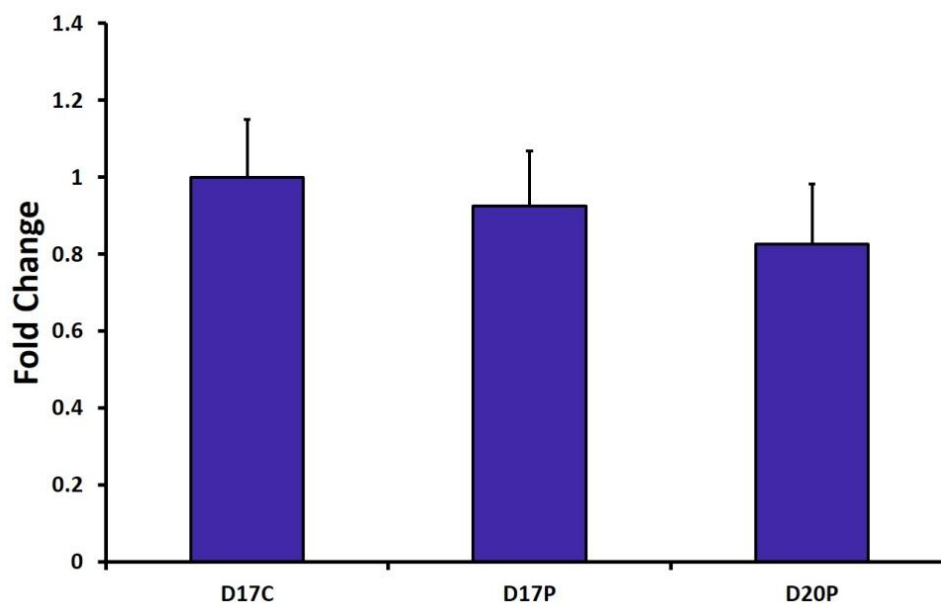


**Figure 8:** Relative *AHR* expression in the endometrium of D17C, D17P, and D20P heifers. There was no difference ( $P > 0.10$ ) in the relative *AHR* mRNA abundance between statuses.

### Western Blot

Total cellular protein (50  $\mu\text{g}$ ) extracted from the endometrium was separated by polyacrylamide gradient gel electrophoresis, transferred to nitrocellulose and detected with a monoclonal anti-human *AHR* antibody. A duplicate polyacrylamide gel was stained with coomassie brilliant blue R-250 dye which confirmed the equality of protein loading between samples (Figure 9). A band was also visualized in the gel lane corresponding to in vitro

translated murine AHR, the positive control used for AHR detection on the nitrocellulose membrane incubated with AHR antibody.

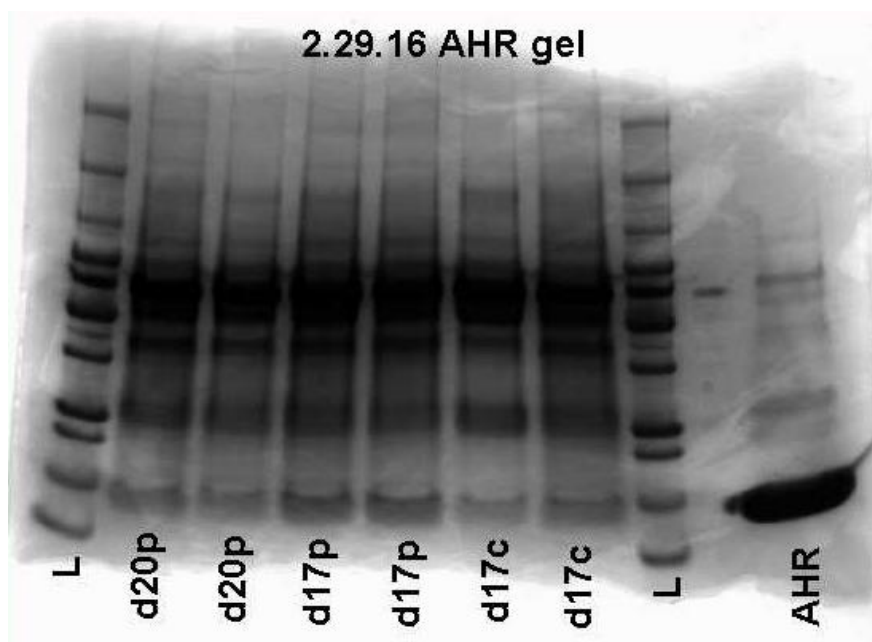


**Figure 9:** Image of polyacrylamide gradient gel electrophoresis with endometrial proteins. The gel was stained with coomassie brilliant blue R-250 dye to confirm protein loading. The AHR lane contained positive control in vitro translated murine AHR protein.

AHR protein was visualized at approximately 96 kDa using a ChemiDoc XRS system (Figure 10). Preliminary experiments using nonfat dry milk as a nonspecific blocking agent prior to incubation of the membrane with AHR antibody did not result in usable results. Using bovine serum albumin (BSA) as blocking agent reduced the number of bands detected and resulted in optimal band intensity of the positive control. We were unable to establish the identity of all the crossreacting bands, but we did detect a band that migrated at a molecular weight consistent with the human AHR protein (molecular weight=96,147 Daltons). A band at 96 kDa was visualized in all of the endometrial protein samples studied (n=6), with two heifers from each experimental group (D17C, D17P, and D20P) analyzed.

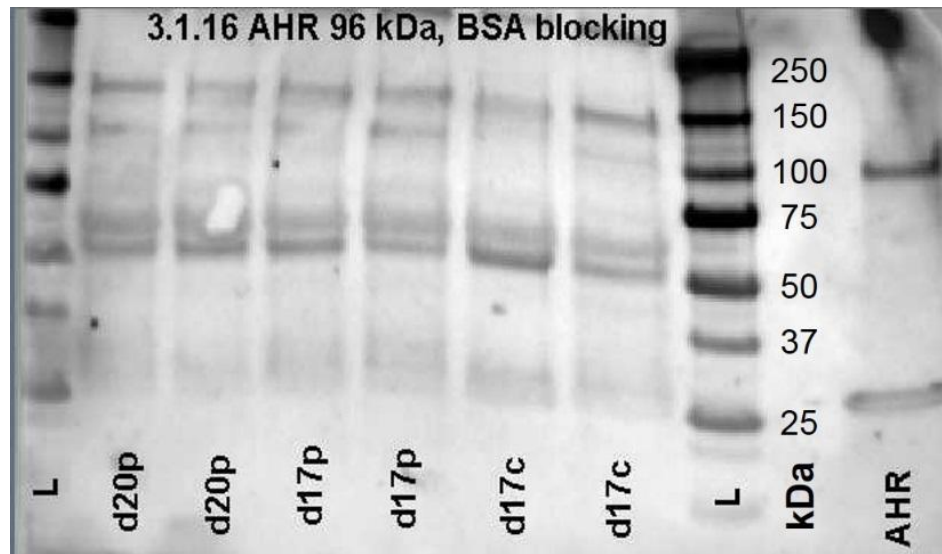


**Figure 10:** Western blot of endometrial proteins incubated with anti-human AHR antibody. Positive control was in vitro translated murine AHR. Molecular weight ladder (L) was used to estimate AHR protein at the expected 96 kDa. A band of similar molecular weight was detected in all of the samples examined. However, several cross reacting bands were detected and their identity was not determined.

### Immunohistochemistry

Images of positive staining for AHR protein on tissue sections were visualized by red secondary antibody staining using a red fluorescence filter (U-N41004, Olympus) on a fluorescent microscope (Figure 11). All images were captured at 833.33 milliseconds of exposure. Images of cell nuclei stained with DAPI were captured using a blue fluorescence filter (U-MNU2, Olympus) at varying exposures. Three images of AHR immunofluorescence and DAPI staining were captured from the luminal epithelium (LE), shallow stroma (SS), shallow glands (SG), deep glands (DG), and myometrium (M) for each of the two tissue sections analyzed per heifer.

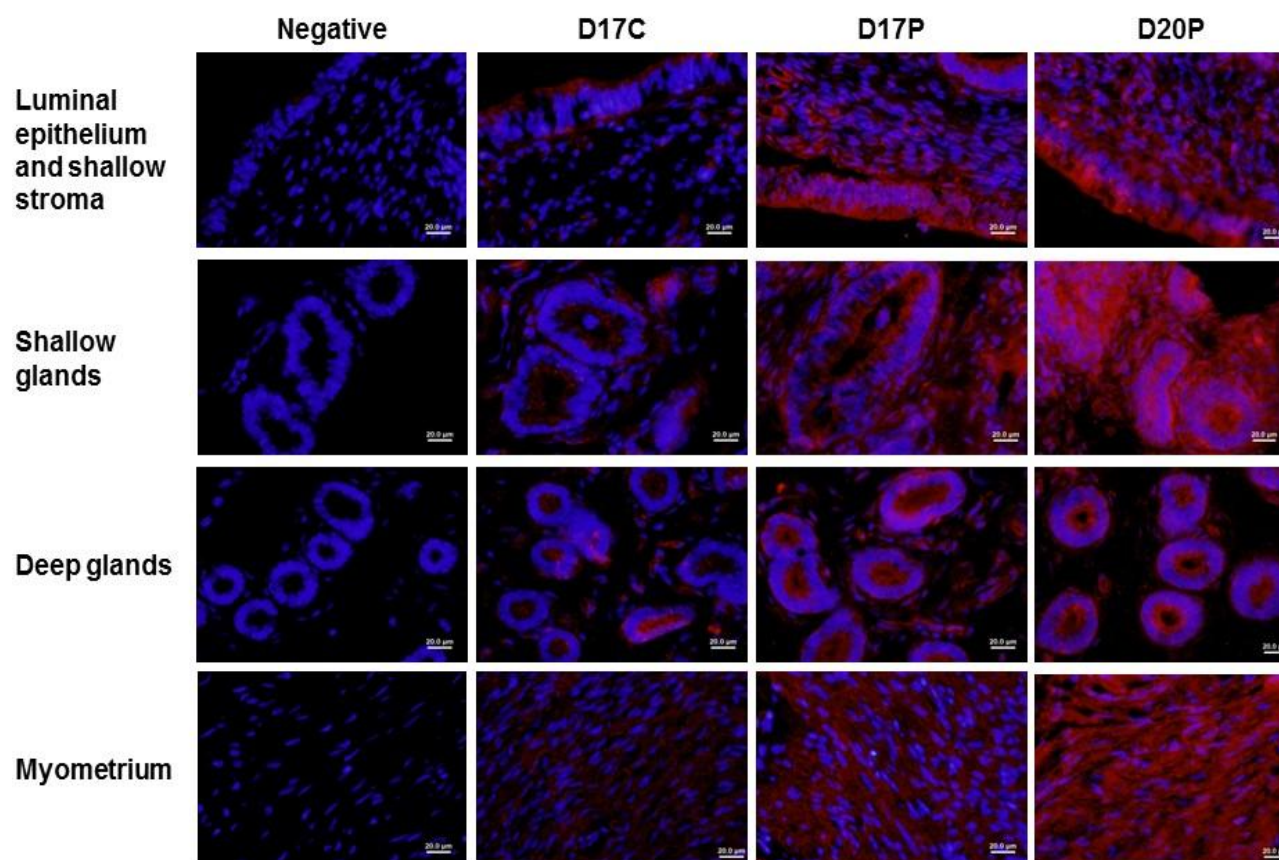


**Figure 11:** Representative uterine AHR immunofluorescent images.

Uterine sections (5  $\mu\text{m}$ ) were labeled (red) with a mouse anti-human AHR monoclonal antibody (MA1-514, Thermo Fisher Scientific, Rockford, IL) and negative controls were labeled with IgG1 negative isotype antibody (MCA928, AbD Serotec, Raleigh, NC). Cell nuclei stained with DAPI are visible in blue. Images represent a cross section of the uterus from the luminal epithelium (top images, site of embryonic attachment) outward to the myometrium (bottom images). Labeling was visualized using an Olympus BX-51 fluorescent microscope (Olympus, Tokyo, Japan) and images were taken using DP71 image capture software. D17P and D20P had a greater percent area of AHR labeling in the shallow stroma ( $P = 0.05$ ) and tended to have greater labeling in the myometrium ( $P = 0.06$ ) compared to D17C.

The average labeling intensity and percent area labeled for each tissue region per heifer was determined using NIH ImageJ software and was statistically analyzed using the Mixed procedures of SAS (Ver. 9.3) and orthogonal contrasts (Figure 12). Differences in percent labeling intensity were identified in the shallow stroma ( $P = 0.05$ ) and a tendency for a difference in the myometrium ( $P = 0.06$ ) was detected, with D17P and D20P having a higher AHR protein

concentration in these regions. There were no differences in percent area labeled in the total uterine wall ( $P > 0.10$ ), luminal epithelium ( $P > 0.10$ ), shallow glands ( $P > 0.10$ ), or deep glands ( $P > 0.10$ ) among groups, however in each of these areas the estimates of percent area labeled were changing similarly.

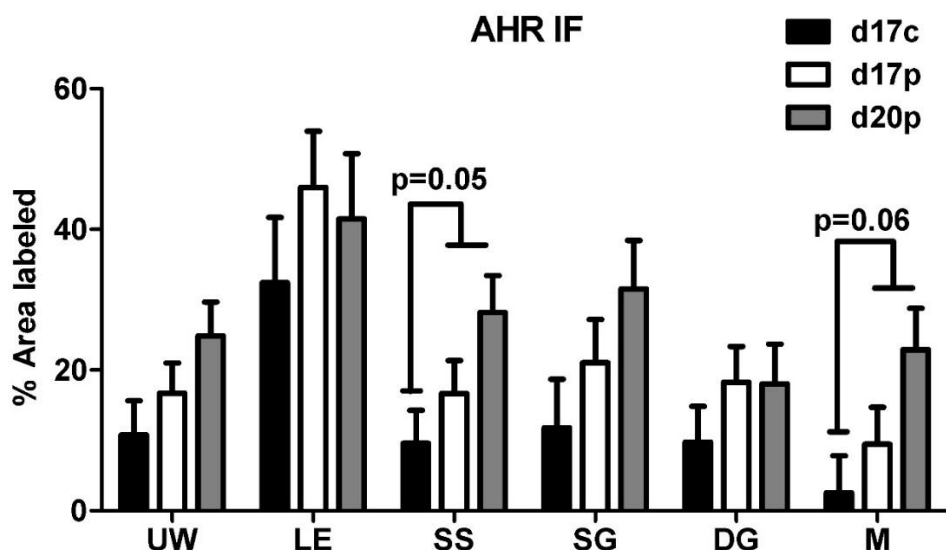


**Figure 12:** Percent area labeled for the AHR in uterine wall (UW), luminal epithelium (LE), shallow stroma (SS), shallow glands (SG), deep glands (DG) and myometrium (M). D17P and D20P heifers had a higher percent area labeled in the shallow stroma ( $P = 0.05$ ) and a tendency for greater labeling in the myometrium ( $P = 0.06$ ) compared to D17C.

### Flow Cytometry

Proliferation of peripheral blood immune cells in response to kynurenine in vitro was measured by flow cytometry. Mean CFSE labeling intensity, analyzed by FlowJo software, is an indicator of positive cell proliferation with lower intensity reflecting greater proliferation. Analysis of flow cytometry data indicated there was no effect of kynurenine on immune cell proliferation at the observed doses of 25-400  $\mu\text{M}$ , as proliferation at these doses was similar to the controls. Consistent proliferation of ConA stimulated cells also cultured with kynurenine

confirmed the PBMC were capable of responding to stimulation in culture, but did not show a response to kynurenine (Figure 13).

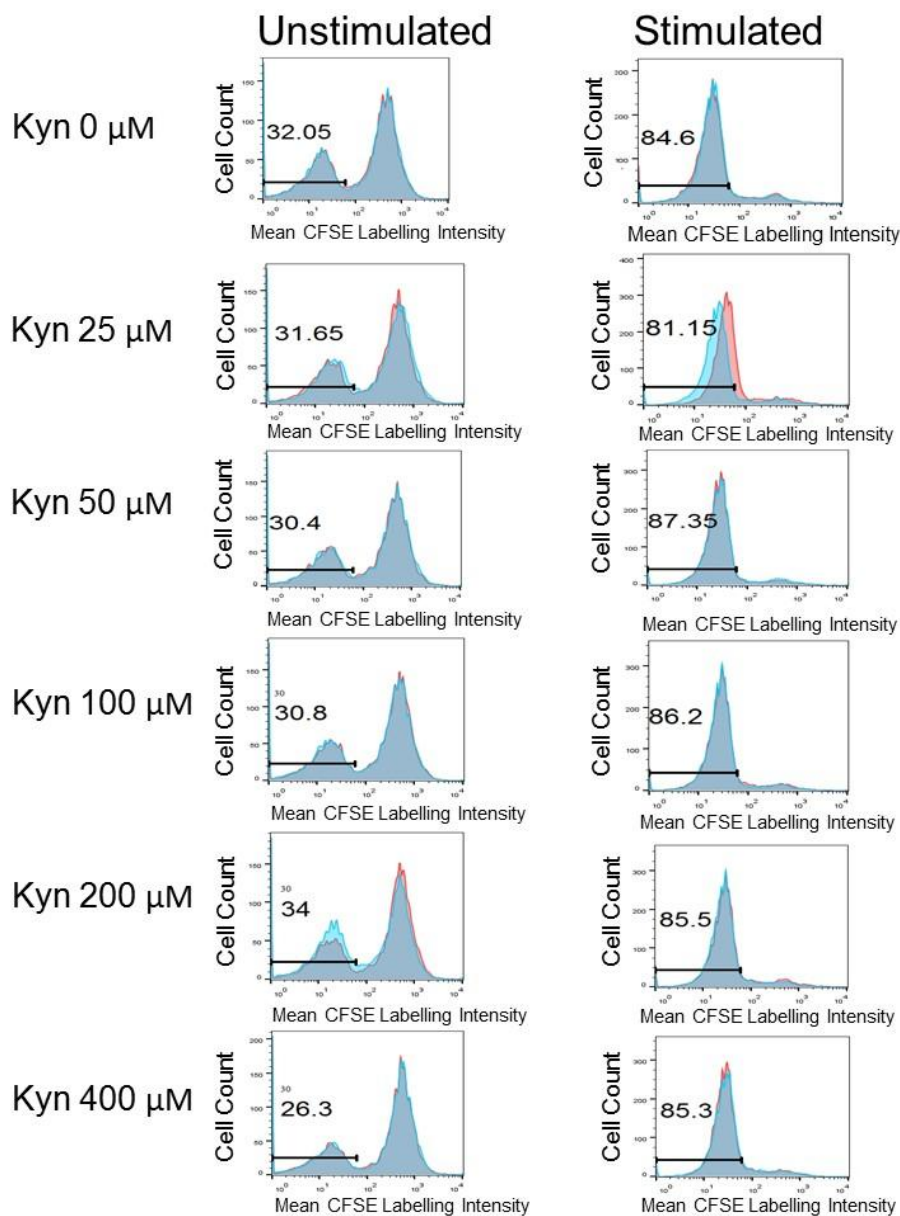


**Figure 13:** Effects of kynurenine on PBMC proliferation with or without ConA.

Cells were cultured for 72 hours in RPMI-1640 with 0.1% ITS and 0.2% gentamycin. Percent proliferation was determined using a Guava EasyCyte Plus and analyzed using FlowJo software. No significant difference in mean CFSE labelling intensity was observed between unstimulated cells cultured without kynurenine and unstimulated cells cultured with 25-400 μM kynurenine. Proliferation in response to ConA confirmed the proliferative potential of the cells and the lack of effect of kynurenine at the concentrations studied.

## DISCUSSION

This objective of this study was to identify if AHR mRNA and protein were expressed in the bovine uterus and to determine if AHR expression was altered in response to conceptus signaling. Results of polymerase chain reaction and gel electrophoresis indicate mRNA for *AHR* was present in all three groups studied. An abundant band was visible at the expected 164 base pairs (bp), which corresponded to the expected amplicon length of *AHR*. This finding was supported by sequencing of one cDNA amplicon of a day 20 pregnant heifer, which revealed 97% sequence similarity to *Bos taurus AHR* (NCBI Gene #280714). This supports our hypothesis that *AHR* gene is transcribed in the bovine endometrium. This is the first study to identify mRNA expression for *AHR* in the uterus of dairy cattle.

Results of qPCR analysis indicated that *AHR* is highly expressed in all three groups studied within the endometrium (see appendix for *AHR* Ct values). Critical threshold values for *AHR* fell in the range of 25-30 Ct, similar to those of *RPL19* for the same heifers (see appendix for *RPL19* Ct values). Statistical analysis using PROC Mixed and orthogonal contrasts found no difference in *AHR* or *RPL19* expression among day 17 cyclic, day 17 pregnant, and day 20 pregnant heifers. Therefore, the results of qPCR analysis studies do not support the hypothesis that *AHR* mRNA is more highly expressed in pregnant heifers. Although there was no difference in expression of *AHR*, gene expression is not necessarily a predictor for concentration of the protein encoded by the gene, because many avenues of post-transcriptional gene regulation exist. Therefore, Western blot and immunofluorescence analysis are necessary to confirm whether the *AHR* protein is present in the uterus and if a difference in the temporal or spatial expression of *AHR* protein exists.

Western blot analysis of protein isolated from the endometrium confirmed AHR protein was present in the endometrium of all three groups studied. The gel stained with coomassie brilliant blue confirmed that protein loading was similar for each of the samples and it showed the expected AHR protein band in the positive control. Western blot analysis revealed a protein at 96 kDa in the positive control, which corresponds to the expected molecular weight of AHR of 96,147 Da. A similar sized band was detected in the endometrial samples, however there were a number of cross reacting bands whose identity was not confirmed. Definitive identification of these other bands as isoforms of AHR would require band excision and sequencing, which was beyond the scope of this experiment. These results are consistent with the qPCR analysis which showed that *AHR* mRNA was expressed in all three groups studied.

Indirect immunofluorescence analysis was used to describe the temporal and spatial expression of AHR protein in the uterus. Results showed no difference in percent area labeled for AHR across the entire uterine wall. However, AHR expression was more abundant in the shallow glands ( $P = 0.05$ ) and tended to be more abundant in the myometrium ( $P = 0.06$ ) in pregnant compared to cyclic heifers. This pattern of AHR expression differed somewhat from previous work from our lab showing abundant expression of IDO in the luminal epithelium of D17P heifers but a subsequent reduction in D20P. Therefore, these results could suggest kynurenine production from IDO may only be involved in initial activation of AHR, as AHR is found in high concentrations within the luminal epithelium of pregnant heifers in day 17 through day 20.

In all images of all groups, AHR could be visualized in the nucleus as well as the cytoplasm, however, no attempt was made to quantify nuclear localization. Localization in the nucleus indicates the receptor is transcriptionally active. Results indicate the concentration of the

protein is highest in all three groups in the luminal epithelium, the uterine region in direct contact with the conceptus. This finding may indicate AHR is a key protein in facilitating early embryonic attachment or development. Additionally, it is higher in the shallow stroma of pregnant heifers, which supports the hypothesis that AHR may have a role in early pregnancy because this tissue region is near the site of placental attachment. These results are consistent with the finding that AHR and ARNT are upregulated in the luminal and glandular epithelium of pregnant rabbits at the time of blastocyst attachment (Tscheudschilsuren *et al.*, 1999).

The results of the cell culture experiment are not consistent with our hypothesis that cells cultured with kynurenine would exhibit reduced cell proliferation relative to controls. T helper cells comprise a significantly larger proportion of PBMC than T regulatory cells. Therefore, we expected PBMC cultured with kynurenine to exhibit a reduction in proliferation compared to cells cultured without kynurenine. Flow cytometric analysis indicates kynurenine did not have a measurable effect on proliferation at concentrations ranging from 25-400  $\mu$ M. The lack of effect was consistent because labeling intensity of CFSE, an indicator of cell proliferation, ranged between 26-32% in all unstimulated cells. Consistent proliferation among ConA stimulated control cells was also evident, with CFSE labeling intensity ranging from 81-87%. This indicates the cells were capable of responding to stimulation, but did not proliferate differently in the presence of kynurenine. These results may indicate kynurenine does not have an effect on differentiation of naïve T cells in cattle. Finally, the hypothesis was that these mechanisms occur at the fetal-maternal interface, but due to limitations on obtaining uterine immune cells, we were unable to test this hypothesis directly in this experiment. Other results from our lab suggest that uterine immune cells and peripheral blood immune cells respond differently to conceptus

signaling. Overall, results from this study do not support the hypothesis that kynurenine affects proliferation of naïve T cells in dairy cattle.

## CONCLUSIONS AND SIGNIFICANCE

The overall goal of this study was to characterize the expression and localization of AHR in the endometrium and to examine the effect of kynurenine on immune cell proliferation. This study is the first to identify both AHR mRNA and protein in the uterus of dairy cattle. Although no differences in expression of AHR were detected between groups, its abundant expression in all groups suggests this receptor has a physiological function in the uterus of dairy cattle. The high concentration of AHR in the luminal epithelium may support that its activation is regulated by the conceptus or through IDO induced kynurenine production, which is highly localized to this region in D17P heifers. This would support our overall hypothesis that kynurenine activates AHR and initiates signaling through this pathway. However, a larger sample size should be studied before stronger conclusions are made regarding the function of AHR in pregnancy due to differences in AHR mRNA and protein concentrations identified between pregnant and cycling dairy heifers.

Although no measurable effect of kynurenine on PBMC proliferation was observed, the dose response experiment should be repeated with different immune cell types to gain a more complete understanding of whether this metabolite has an effect on bovine immune cell proliferation. Repeating the experiment with purified T cells would provide results on the effect of kynurenine on effector cell proliferation specifically. It would also be important to determine if kynurenine affected the number or function to T regulatory cells in the uterus during early pregnancy. Additionally, culturing uterine immune cells with kynurenine could produce different results than PBMC, because uterine immune cells were shown to respond differently than peripheral blood immune cells to various stimuli (Slukvin *et al.*, 1994).

Nutritional management applications are viewed as viable approaches to improve fertility on dairy farms (Thatcher *et al.*, 2010). Dairy cattle rations can be formulated to include certain additives that have pro-inflammatory or anti-inflammatory properties. For example, dairy producers currently modify diets to enrich omega-6 or omega-3 fatty acids to achieve a pro- or anti-inflammatory effect, respectively (Thatcher *et al.*, 2011). Applications from this project may be devised to improve reproductive performance and profitability if kynurenine is identified as an anti-inflammatory amino acid metabolite. During pregnancy, it may be of advantage to formulate dairy cattle rations with anti-inflammatory ingredients to modify the status of uterine immune cells to promote successful establishment of pregnancy.

## APPENDIX

**Table 1:** Critical threshold (Ct) values from *AHR* and *RPL19* qPCR

<b>Heifer Number</b>	<b>Status</b>	<b>C<sub>T</sub> AHR</b>	<b>C<sub>T</sub> RPL19</b>
10864	D17C	29.52	29.45
781	D17C	30.36	31.14
445	D17C	27.53	29.01
706	D17C	27.86	28.85
687	D17C	24.92	24.76
822	D17C	26.87	27.078
773	D17C	26.22	26.96
54	D17C	26.89	26.96
304	D17C	26.87	27.07
2	D17P	29.87	26.99
3	D17P	26.34	27.17
4	D17P	27.01	27.92
5	D17P	31.28	31.29
211	D17P	26.13	26.12
269	D17P	28.28	29.01
701	D17P	29.36	29.65
707	D17P	29.44	30.25
863	D17P	27.04	28.02
50	D20P	25.94	25.89
702	D20P	27.57	28.46
708	D20P	28.08	27.95
712	D20P	29.89	30.13

**REFERENCES**

1. Bascom, SS, Young AJ. "A Summary of the Reasons Why Farmers Cull Cows." *J. Dairy Sci.* 1998; 81(8):2299-2305.
2. Gröhn, YT, Rajala-Schultz, PJ. "Epidemiology of reproductive performance in dairy cows." *Anim. Reprod. Sci.* 2000; 2:605-614.
3. Hansen PJ. "Improving dairy cow fertility through genetics." In: 44th Florida Dairy Production Conference; May 1, 2007; Gainesville, FL. 23-29.
4. Weigel KA. "Prospects for improving reproductive performance through genetic selection." *Anim. Reprod. Sci.* 2006; 96:323–330.
5. "Fertility: The fundamental element of reproduction." Dairy Cattle Reproduction Council (DCRC) Newsletters 2009; 3(4).
6. Bello, NM, Stevenson, JS, Tempelman, RJ. "Invited review: Milk production and reproductive performance: Modern interdisciplinary insights into an enduring axiom." *J. Dairy Sci.* 2012; 95:5461–5475.
7. Vassilev N, Yotov S, and Dimitrov F. "Incidence of early embryonic death in dairy cows." *Trakia Journal of Sciences* 2005; 3(5):62–64.
8. Santos, JE, Thatcher, WW, Chebel RC, Cerri RL, Galvao KN. "The effect of embryonic death rates in cattle on the efficacy of estrus synchronization programs." *Anim. Reprod. Sci.* 2004; 11(3);254-269.
9. Geary, TW. "Management Strategies to Reduce Embryonic Loss." *Proc Range Beef Cow Symposium.* October 3-4, 2006.
10. Reynolds, LP, Ferrell, CL, Nienaber, JA, Ford, SP. "Effects of Chronic Environmental Heat Stress on Blood Flow and Nutrient Uptake by the Uterus and Fetus of the Pregnant

- Cow.” Roman L. Hruska U.S. Meat Anim. Res. Center and Univ. of Nebraska 1985; 77–79.
11. Putney, DJ, Torres, CA, Thatcher, WW, Plante, C, Drost, M. “Modulation of uterine prostaglandin biosynthesis by pregnant and nonpregnant cows at day 17 postestrus in response to in vivo and in vitro heat stress.” *Anim. Reprod. Sci.* 1989; 20(1):31-47.
  12. Walsh, SW, Williams, EJ, Evans, ACO. “A review of the causes of poor fertility in high milk producing dairy cows.” *Anim. Reprod. Sci.* 2011; 123(3-4):127-138.
  13. Kirby, CJ, Thatcher WW, Collier RJ, Simmen FA, Lucy MC. “Effects of growth hormone and pregnancy on expression of growth hormone receptor, insulin-like growth factor-I, and insulin-like growth factor binding protein-2 and -3 genes in bovine uterus, ovary, and oviduct.” *Biol. Reprod.* 1996; 55(5):996–1002.
  14. Ahmadzadeh, A, Frago, F, Shafii, B, Dalton, JC, Price, EJ, McGuire, MA. "Effect of clinical mastitis and other diseases on reproductive performance of Holstein cows." *Anim. Reprod. Sci.* 2009; 112:273–282.
  15. Fourichon, C, Seegers, H, Malher, X. “Effect of disease on reproduction in the dairy cow: a meta-analysis. *Theriogenology* 2000; 53:1729-1759.
  16. LeBlanc, SJ. "Postpartum uterine disease and dairy herd reproductive performance: a review." *Vet. J.* 2008; 176:102–114.
  17. Santos, JEP, Ribeiro, ES. "Impact of animal health on reproduction of dairy cows." *Anim. Reprod.* 2014; 11(3):254-269.
  18. Brooks, K, Burns, G, Spencer, T. "Conceptus elongation in ruminants: roles of progesterone, prostaglandin, interferon tau and cortisol." *Journal of Animal Science and Biotechnology* 2014; 5(1):53.
  19. Ott TL, Gifford CA. “Effects of early conceptus signals on circulating immune cells: lessons from domestic ruminants.” *Am. J. Reprod. Immunol.* 2010; 64:245-254.

20. Bazer, FW, Kim, J, Song, G, Satterfield, MC, Johnson, GA, Burgardt, RC, Wu, G. "Uterine environment and conceptus development in ruminants." *Anim. Reprod.* 2012; 9(3):297-304.
21. Baba T, Mimura J, Nakamura N, Harada N, Yamamoto M, Morohashi K, Fujii-Kuriyama Y. "Intrinsic function of the aryl hydrocarbon (dioxin) receptor as a key factor in female reproduction." *Mol. Cell. Biol.* 2005; 25(22):10040-10051.
22. Jiang, Y, Wang, K, Fang, R, Zheng, J. "Expression of Aryl Hydrocarbon Receptor in Human Placentas and Fetal Tissues." *Journal of Histochemistry & Cytochemistry* 2010; 58(8):679-685.
23. Hernandez-Ochoa, I, Karman, BN, Flaws, JA. "The role of the aryl hydrocarbon in the female reproductive system." *Biochemical Pharmacology* 2008; 77(4):547-59.
24. Nebert DW, Dalton TP, Okey AB, Gonzalez FJ. "Role of aryl hydrocarbon receptor-mediated induction of the CYP1 enzymes in environmental toxicity and cancer." *J. Biol. Chem.* 2004; 279(23):23847-50.
25. Pocar P, Fischer B, Klonisch T, Hombach-Klonisch S. "Molecular interactions of the aryl hydrocarbon receptor and its biological and toxicological relevance for reproduction." *Reproduction* 2005; 129:379–389.
26. Mezrich, JD, Fechner, JH, Zhang, X, Johnson, BP, Burlingham, WJ, Bradeld, CA. "An Interaction between Kynurenine and the Aryl Hydrocarbon Receptor Can Generate Regulatory T Cells." *Journal of Immunology* 185(6):3190-3198.
27. Shin, JH, Zhang, L, Murillo-Sauca, O, Kim, J, Kohrt, HE, Bui, JD, Sunwoo, JB. "Modulation of natural killer cell antitumor activity by the aryl hydrocarbon receptor." *Proc. Natl. Acad. Sci.* 2013; 110:12391–12396.
28. Sakaguchi S, Miyara M, Costantino CM, Hafler DA. "FOXP3+ regulatory T cells in the human immune system." *Nat. Rev. Immunol.* 2010; 10:490–500.

29. Stevens, EA, Bradfield, CA. Immunology: T cells hang in the balance. *Nature* 2008; 453(7191):46–47.
30. Munn, DH, Mellor, AL. "Indoleamine 2,3-dioxygenase and tumor-induced tolerance." *J. Clin. Invest.* 2007; 117(5):1147–1154.
31. Pocar, P, Augustin, R, Fishcer, B. "Constitutive Expression of CYP1A1 in Bovine Cumulus Oocyte-Complexes in Vitro: Mechanisms and Biological Implications." *Endocrinology* 2003; 145(4):1594-601.
32. Kluxen, FM, Höfer, N, Kretzschmar, G, Gisela H. Degen, GH, Diel P. "Cadmium modulates expression of aryl hydrocarbon receptor-associated genes in rat uterus by interaction with the estrogen receptor." *Toxicogenomics* 2011; 86(4):591-601.
33. Ruocco, MG, Chaouat, G, Florez, L, Bensussan, A, Klatzmann, D. "Regulatory T-cells in pregnancy: historical perspective, state of the art, and burning questions." *Front. Immunol.* 2014; 21(5):389.
34. Cady, SG, Sono, M. "1-Methyl-dl-tryptophan, beta-(3-benzofuranyl)-dl-alanine (the oxygen analog of tryptophan), and beta-[3-benzo(b)thienyl]-dl-alanine (the sulfur analog of tryptophan) are competitive inhibitors for indoleamine 2,3-dioxygenase." *Arch. Biochem. Biophys.* 1991. 291:326–333.
35. Abbott, BD, Schmid, JE, Pitt, JA, Buckalew, AR, Wood, CR, Held, GA, Diliberto, JJ. "Adverse Reproductive Outcomes in the Transgenic Ah Receptor-Deficient Mouse." *Toxicology and Applied Pharmacology* 1999; 155(1):62-70.
36. Tscheudschilsuren G1, Hombach-Klonisch S, Küchenhoff A, Fischer B, Klonisch T. "Expression of the arylhydrocarbon receptor and the arylhydrocarbon receptor nuclear translocator during early gestation in the rabbit uterus." *Toxicol. Appl. Pharmacol.* 1999; 160(3):231-7.

37. Slukvin II, Chernyshov VP, Merkulova AA, Vodyanik MA, Kalinovsky AK.  
"Differential expression of adhesion and homing molecules by human decidual and peripheral blood lymphocytes in early pregnancy." *Cell Immunol.* 1994; 158(1):29-45.
38. Thatcher WW, Santos JE, Silvestre FT, Kim IH, Staples CR. "Perspective on physiological/endocrine and nutritional factors influencing fertility in post-partum dairy cows." *Reprod. Domest. Anim.* 2010; Suppl. 3(45):2-14.
39. Thatcher WW, Santos JE, Staples CR. "Dietary manipulations to improve embryonic survival in cattle." *Theriogenology* 2011; 76(9):1619-31.

## **ACADEMIC VITA**

Michelle Christina Hartzell  
111 Hartzell Lane  
Slippery Rock, PA, 16057  
mhartzell07@gmail.com

### **Education**

---

The Pennsylvania State University  
Schreyer Honors College  
Bachelor of Science in Animal Science, Spring 2016  
Thesis title: Role of the Aryl Hydrocarbon Receptor in Endometrium of Dairy Heifers During the Estrous Cycle and Early Pregnancy  
Thesis Supervisor: Troy L. Ott

### **Experience**

---

Dairy Cattle Reproductive Physiology Undergraduate Research (2014-2016)  
Rainbow Babies and Children's Hospital Pediatric Research Internship (Summer 2015)

### **Involvement**

---

Penn State Dairy Science Club (2012-2016)  
President, Treasurer

Morrill Chapter of Alpha Zeta Fraternity (2013-2016)  
Chronicler, Community Service Chairperson

American Dairy Science Association - Student Affiliate Division (2014-2015)  
Officer at Large

Penn State Ag Advocates (2013-2016)

### **Honors and Awards**

---

Penn State University Student Leader Scholarship  
American Dairy Science Association (ADSA) Student Scholarship Award  
American Society of Animal Science (ASAS) Undergraduate Scholarship Recognition Award  
College of Agricultural Sciences Alumni Society Internship Award  
Gamma Sigma Delta Honorary Society in Agricultural Sciences  
Coaly Leadership Honor Society in Agricultural Sciences  
College of Agricultural Sciences Undergraduate Research Grant (Spr. & Fall 2015, Spr. 2016)  
3<sup>rd</sup> Place, American Dairy Science Association (ADSA) Undergraduate Poster Competition  
2<sup>nd</sup> Place, ADSA Northeast Student Affiliate (NESA) Original Research Paper Competition  
ADSA Northeast Student Affiliate (NESA) Outstanding Senior Award  
College of Agricultural Sciences Ag Woman of the Year